

## Theory of the excitonic spin-density-wave state in iron pnictides

P. M. R. Brydon\* and C. Timm†

*Institut für Theoretische Physik, Technische Universität Dresden, 01062 Dresden, Germany*  
(Received 9 March 2009; revised manuscript received 22 April 2009; published 11 May 2009)

We examine the appearance of a spin-density wave in the FeAs parent compounds due to an excitonic instability. Using a realistic four-band model, we show that the magnetic state depends very sensitively on the details of the band structure. We demonstrate that an orthorhombic distortion of the crystal enhances the stability of the antiferromagnetic order.

DOI: [10.1103/PhysRevB.79.180504](https://doi.org/10.1103/PhysRevB.79.180504)

PACS number(s): 75.30.Fv, 75.10.Lp

### I. INTRODUCTION

The superconductivity of materials containing FeAs layers is currently receiving much attention. Like the cuprates, these systems become superconducting upon chemical doping of an antiferromagnetic (AF) parent compound, specifically ReFeAsO (Re is a rare-earth ion) or AeFe<sub>2</sub>As<sub>2</sub> (Ae is an alkaline-earth ion).<sup>1,2</sup> Intriguingly, the AF state occurs only in the presence of an orthorhombic distortion of the crystal, which fixes the AF ordering direction.<sup>3,4</sup> The likely role of spin fluctuations in producing the superconductivity has led to intense scrutiny of the AF phase. The relatively small value of the moment at Fe sites,<sup>3-5</sup> metallic transport properties,<sup>5,6</sup> and observations of reconstructed Fermi surfaces<sup>7,8</sup> provide strong evidence that the AF state is a spin-density wave (SDW) arising from the nesting of electron and hole Fermi surfaces,<sup>9-11</sup> in analogy to Cr.<sup>12</sup>

Several authors have suggested an important role for Fe 3*d* orbital physics in the appearance of the SDW.<sup>13-16</sup> On the other hand, it has been argued that a low-energy effective theory without explicit inclusion of orbital effects is sufficient to understand the excitonic instability of the nested electron and hole states.<sup>17-19</sup> As such models have so far only been studied for highly idealized electronic structures with two Fermi surfaces<sup>17-19</sup> instead of the likely four or more,<sup>9,10</sup> it is not clear if they can give the observed magnetic ordering.<sup>3,4</sup> Furthermore, the effect of the orthorhombic distortion in this scenario remains unknown. We address these problems here by studying the appearance of the excitonic SDW in a four-band model of LaFeAsO.<sup>11</sup> Using a mean-field theory, we show that the SDW state is sensitively dependent on the doping and the details of the band structure. In particular, we examine the response of the SDW phase to changes in the ellipticity of the electron pockets, the relative size of the hole pockets, and an orthorhombic distortion of the crystal.

### II. THEORETICAL MODEL

We model the FeAs planes as a two-dimensional (2D) interacting four-band system where two bands have electron-like Fermi surfaces and the other two have hole-like Fermi surfaces. We write the Hamiltonian as

$$\begin{aligned}
 H = & \sum_{n=1,2} \sum_{\mathbf{k}, \sigma} \{ \epsilon_{n\mathbf{k}}^e c_{n\mathbf{k}\sigma}^\dagger c_{n\mathbf{k}\sigma} + \epsilon_{n\mathbf{k}}^h f_{n\mathbf{k}\sigma}^\dagger f_{n\mathbf{k}\sigma} \} \\
 & + \frac{1}{V} \sum_{n=1,2} \sum_{n'=1,2} \sum_{\mathbf{k}, \mathbf{k}', \mathbf{q}} \sum_{\sigma, \sigma'} \{ g_1 c_{n, \mathbf{k}+\mathbf{q}, \sigma}^\dagger c_{n\mathbf{k}\sigma} f_{n', \mathbf{k}'-\mathbf{q}, \sigma'}^\dagger f_{n' \mathbf{k}' \sigma'} \\
 & + g_2 [ c_{n, \mathbf{k}+\mathbf{q}, \sigma}^\dagger c_{n, \mathbf{k}'-\mathbf{q}, \sigma'}^\dagger f_{n' \mathbf{k}' \sigma'}^\dagger f_{n' \mathbf{k} \sigma} \\
 & + c_{n, \mathbf{k}+\mathbf{q}, \sigma}^\dagger f_{n', \mathbf{k}'-\mathbf{q}, \sigma'}^\dagger c_{n\mathbf{k}\sigma} f_{n' \mathbf{k}' \sigma'} \\
 & + f_{n', \mathbf{k}+\mathbf{q}, \sigma}^\dagger c_{n, \mathbf{k}'-\mathbf{q}, \sigma'}^\dagger c_{n\mathbf{k}\sigma} f_{n' \mathbf{k}' \sigma'} \\
 & + f_{n', \mathbf{k}+\mathbf{q}, \sigma}^\dagger f_{n', \mathbf{k}'-\mathbf{q}, \sigma'}^\dagger c_{n\mathbf{k}\sigma} c_{n\mathbf{k}' \sigma'} \} , \quad (1)
 \end{aligned}$$

where  $c_{n\mathbf{k}\sigma}^\dagger$  ( $f_{n\mathbf{k}\sigma}^\dagger$ ) creates a spin- $\sigma$  electron (hole) with momentum  $\mathbf{k}$  in the electron-like (hole-like) band  $n$ . Due to the out-of-plane arrangement of the As ions, the crystallographic unit cell of the FeAs plane contains two Fe ions. Our band structure is given in terms of this unit cell, but when discussing magnetic properties it is more useful to refer only to the Fe lattice, which requires us to “unfold” the Brillouin zone.<sup>9</sup> Assuming crystallographic unit-cell dimensions  $a \times a$ , the bands with electron-like Fermi surface have dispersion  $\epsilon_{n\mathbf{k}}^e = \epsilon_e + t_{e,1} [\cos(k_x a) + \cos(k_y a)] + t_{e,2} \cos\{[k_x + (-1)^n k_y] a\}$ , while for the hole-like bands we have  $\epsilon_{n\mathbf{k}}^h = \epsilon_{h,n} + t_{h,n,1} [\cos(k_x a) + \cos(k_y a)] + t_{h,n,2} \cos(k_x a) \cos(k_y a)$ . In units of eV, we use  $\epsilon_e = 1.544$ ,  $t_{e,1} = 1.0$ ,  $t_{e,2} = -0.2$ ,  $\epsilon_{h,1} = -0.335$ ,  $t_{h,1,1} = 0.24$ ,  $t_{h,1,2} = 0.03$ ,  $\epsilon_{h,2} = -0.512$ ,  $t_{h,2,1} = 0.315$ , and  $t_{h,2,2} = 0.06$ . For electron filling  $n_{el} = 4$ , corresponding to the undoped parent compounds, we find the Fermi surface and dispersion as shown in Figs. 1(a) and 1(b), respectively. Note that the nesting of the hole and electron Fermi surfaces is not perfect since both the shape and the enclosed area differ. Our model reproduces the Fermi surface and low-energy velocities of the band structure proposed in Ref. 11 for LaFeAsO, but unlike Ref. 11 it obeys the correct periodicity of the Brillouin zone.

The interaction terms in Eq. (1) describe a density-density interaction and correlated transitions between the electron and hole bands, with contact potentials  $g_1 > 0$  and  $g_2 > 0$ , respectively. These naturally arise in the low-energy effective theory of a multiorbital model<sup>18</sup> and are responsible for the excitonic instability.<sup>12,20-23</sup> Although a rich variety of excitonic phases is possible, here the SDW state has the largest effective coupling constant  $g_s = g_1 + 2g_2$ .<sup>18,22</sup> At mean-field level, we therefore decouple the interactions via the

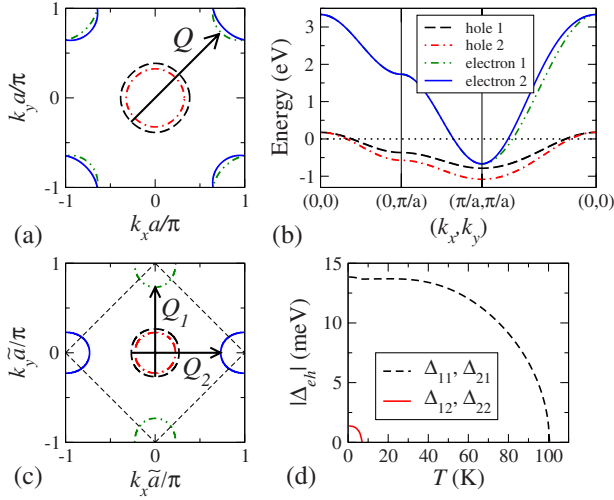


FIG. 1. (Color online) (a) Fermi surface with nesting vector  $\mathbf{Q}$  at filling  $n_{el}=4$  and (b) dispersion of the electron and hole bands in the physical Brillouin zone. (c) Fermi surface in the unfolded Brillouin zone, showing orthogonal nesting vectors  $\mathbf{Q}_1$  and  $\mathbf{Q}_2$ . The dashed square is the physical Brillouin zone.  $\tilde{a}=a/\sqrt{2}$  is the nearest-neighbor Fe-Fe distance. (d) Variation of the excitonic gaps with temperature at  $n_{el}=4$ .

introduction of the real SDW excitonic averages  $\Delta_{eh} = (g_s/V) \sum_{\mathbf{k}} \sum_{\sigma} \langle c_{e,\mathbf{k}+\mathbf{Q},\sigma}^\dagger c_{h,\mathbf{k},\sigma} \rangle$  where  $\mathbf{Q}=(\pi/a, \pi/a)$  is the nesting vector [see Fig. 1(a)] and  $e(h)$  takes values of 1 or 2 to index the electron (hole) bands. Although  $\Delta_{eh}$  is the order parameter of the SDW state,<sup>12,20</sup> it is only indirectly related to the staggered magnetization.<sup>22</sup> As shown in Fig. 1(c), each electron pocket is mapped to a different  $X$  point of the enlarged Brillouin zone upon unfolding,<sup>9</sup> and  $\Delta_{1h}$  and  $\Delta_{2h}$  hence involve orthogonal nesting vectors  $\mathbf{Q}_1$  and  $\mathbf{Q}_2$  with respect to the Fe sites, respectively. When both  $\Delta_{1h}$  and  $\Delta_{2h}$  are nonzero, therefore, the magnetization is the superposition of two orthogonal SDW states, each with stripe-like ordering.<sup>14</sup>

After decoupling the interaction terms, we obtain the equilibrium mean-field solution by numerical minimization of the free energy  $F$  with respect to the  $\Delta_{eh}$ . This was calculated over the 2D Brillouin zone with at least a  $1000 \times 1000$   $\mathbf{k}$ -point mesh. Throughout our work we set the effective SDW coupling constant to be  $g_s=0.84$  eV, as at  $n_{el}=4$  this gives a partially gapped Fermi surface in the SDW state with reasonable critical temperatures: as shown in Fig. 1(d) we find that  $\Delta_{e1}$  is nonzero below  $T_{SDW1}=100$  K, while  $\Delta_{e2}$  appears below  $T_{SDW2}=6.5$  K. When all four averages are nonzero, we find the inequality  $\Delta_{11}\Delta_{12}\Delta_{21}\Delta_{22}<0$ ; when only two  $\Delta_{eh}$  are present, their signs are independent.

### III. ELLIPTICITY OF THE ELECTRON POCKETS

As seen in Fig. 1(d), both electron bands participate in the excitonic instability at  $n_{el}=4$ . This corresponds to a  $\mathbf{Q}_1+\mathbf{Q}_2$  SDW, whereas only a single- $\mathbf{Q}$  SDW is experimentally observed.<sup>3,4</sup> It has previously been noted that these two SDW phases should lie at similar energies,<sup>16</sup> and so it is interesting to see whether slight changes in the band structure can sta-

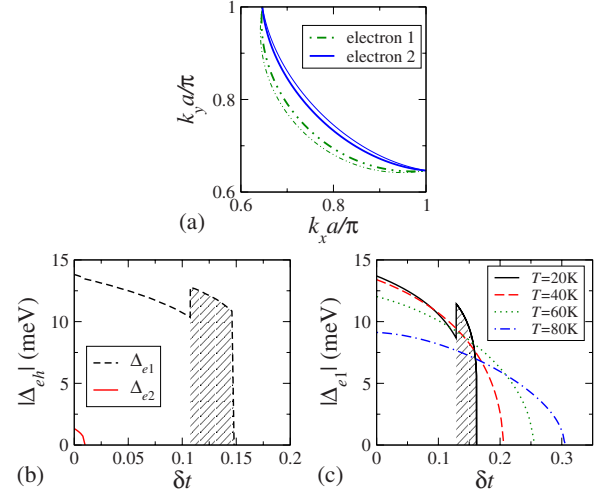


FIG. 2. (Color online) (a) Electron Fermi surfaces at  $\delta t=0.2$  (thick lines) compared to  $\delta t=0$  (thin lines). (b) Variation of  $\Delta_{eh}$  with  $\delta t$  at  $T=1$  K. (c) Variation of  $\Delta_{e1}$  with  $\delta t$  at various temperatures. In (b) and (c) shading beneath the curve indicates a single- $\mathbf{Q}$  solution.

bilize a single- $\mathbf{Q}$  state. This might be achieved, for example, by reducing the ellipticity of the two electron pockets so as to enhance their competition for the same states in each hole band. We therefore modify the electron dispersions  $\epsilon_{nk}^e \rightarrow \epsilon_{nk}^e + 2(-1)^n t_{e,2} \delta t \sin(k_x a) \sin(k_y a)$ , where the dimensionless parameter  $\delta t$  controls the ellipticity of the electron pockets. We compare the electron pockets at  $\delta t=0.2$  and  $\delta t=0$  in Fig. 2(a).

We find that even very small values of  $\delta t \neq 0$  can qualitatively alter the mean-field state. The evolution of the  $\Delta_{eh}$  with increasing  $\delta t$  at  $T=1$  K is plotted in Fig. 2(b). Reducing the ellipticity of the electron pockets tends to suppress the excitonic state, with  $\Delta_{e2}$  disappearing before  $\delta t=0.01$  is reached. At  $\delta t=0.108$  the system undergoes a first-order transition from the  $\mathbf{Q}_1+\mathbf{Q}_2$  state into a single- $\mathbf{Q}$  state. A single- $\mathbf{Q}$  state is hence possible at mean-field level by subtle modification of the band structure. Note that the single- $\mathbf{Q}$  states with nesting vectors  $\mathbf{Q}_1$  and  $\mathbf{Q}_2$  are degenerate.<sup>24</sup> Further increasing  $\delta t$ , the system undergoes a first-order transition into the nonmagnetic state at  $\delta t \approx 0.145$ .

The variation of  $\Delta_{e1}$  with  $\delta t$  at higher temperature is shown in Fig. 2(c); in all cases  $\Delta_{e2}=0$ . The first-order transition from the  $\mathbf{Q}_1+\mathbf{Q}_2$  into the single- $\mathbf{Q}$  state only survives up to  $T \sim 30$  K; at higher temperatures, the nonmagnetic state is reached from the  $\mathbf{Q}_1+\mathbf{Q}_2$  phase by a second-order transition. Interestingly, we see that the critical value of  $\delta t$  increases with  $T$ , even as the value of  $\Delta_{e1}$  at  $\delta t=0$  is suppressed. This re-entrant behavior is a generic feature of the phase diagram of the excitonic insulator<sup>12,21</sup> and may indicate the presence of a low- $T$  incommensurate SDW state.<sup>12,19</sup>

### IV. HOLE POCKET DISPARITY

The SDW state is sensitively dependent not only on the shape but also on the size of the Fermi surfaces. This can be seen in two ways: by raising the energy of the second hole

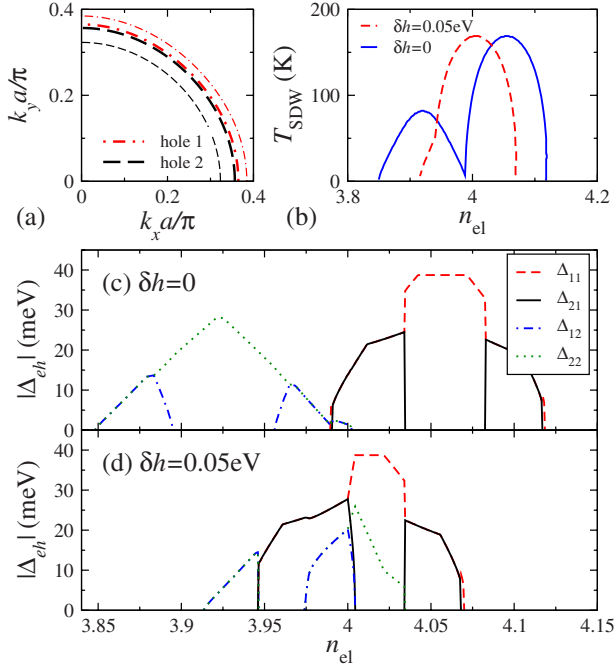


FIG. 3. (Color online) (a) Hole Fermi surfaces at  $\delta h = 0.05$  eV (thick lines) compared to  $\delta h = 0$  (thin lines) at  $n_{el} = 4$ . (b) Dependence of the critical temperature  $T_{SDW}$  of the excitonic phases on electron filling  $n_{el}$  for different values of  $\delta h$ . (c) Variation of the  $\Delta_{eh}$  with  $n_{el}$  at  $T = 1$  K and  $\delta h = 0$ . (d) Same as (c) but for  $\delta h = 0.05$  eV.

band  $\epsilon_{2,\mathbf{k}}^h \rightarrow \epsilon_{2,\mathbf{k}}^h + \delta h$  so that the two hole Fermi surfaces converge together<sup>25</sup> or by varying the filling  $n_{el}$  to improve the nesting between one of the hole Fermi surfaces and the two electron pockets. At  $\delta h = 0.05$  eV, the two hole Fermi surfaces are nearly coincident when  $n_{el} = 4$  [see Fig. 3(a)]. As shown in Fig. 3(b), this causes strong changes in the  $n_{el}$ -dependence of the maximum temperature  $T_{SDW}$  at which at least one  $\Delta_{eh}$  is nonzero. When  $\delta h = 0$ , our model displays two distinct peaks in the  $T_{SDW}$  vs  $n_{el}$  curve, with a sharp minimum at  $n_{el} \approx 3.99$ . This behavior qualitatively disagrees with experiment, which shows only monotonic suppression of  $T_{SDW}$  with electron doping.<sup>1</sup> The behavior of  $T_{SDW}$  at  $\delta h = 0.05$  eV is in much better agreement with experiment, with only a single maximum. The maximum value of  $T_{SDW}$  in both cases is comparable to that in the ReFeAsO systems.<sup>3</sup>

The  $T_{SDW}$  vs  $n_{el}$  curves can be understood by examining the evolution of the  $\Delta_{eh}$  with  $n_{el}$  at  $T = 1$  K, plotted in Fig. 3(c) for  $\delta h = 0$  and in Fig. 3(d) for  $\delta h = 0.05$  eV. Note that the values of the pairs  $(\Delta_{11}, \Delta_{22})$  and  $(\Delta_{21}, \Delta_{12})$  may be swapped at every point. At  $\delta h = 0$ , the two distinct peaks in Fig. 3(b) correspond to a maximum in  $|\Delta_{e1}|$  for electron doping and in  $|\Delta_{e2}|$  for hole doping. The maximum values differ due to different densities of states in the hole bands. These maxima occur when the area enclosed by the hole Fermi surface is the same as that enclosed by each electron Fermi surface. Note that a single- $\mathbf{Q}$  SDW is stable at both maxima.

When  $\delta h = 0.05$  eV, the conditions for  $|\Delta_{e1}|$  and  $|\Delta_{e2}|$  to display a maxima coincide at  $n_{el} = 4$  as the area enclosed by each hole Fermi surface is almost equal. We hence see a complicated coexistence between the four order parameters:

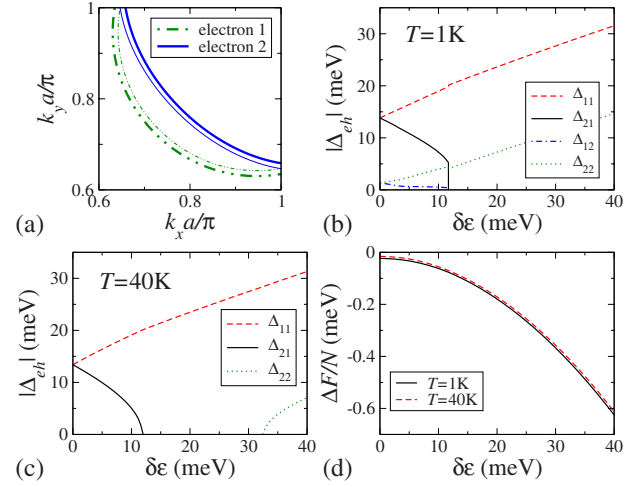


FIG. 4. (Color online) (a) Electron Fermi surface pockets at  $\delta\epsilon = 0.04$  eV (thick lines) compared to  $\delta\epsilon = 0$  (thin lines). (b) Dependence of the  $\Delta_{eh}$  on  $\delta\epsilon$  at  $T = 1$  K. (c) Same as for (b) but at  $T = 40$  K. (d) Difference  $\Delta F = F - F_0$  per site between the free energy  $F$  and its value in the normal state  $F_0$  at  $\delta\epsilon = 0$ .

at weak hole doping, all four  $\Delta_{eh}$  are nonzero; at weak electron doping, the excitonic instability of the two electron bands involve different hole bands. Although  $\Delta_{e1}$  is dominant over most of the doping range, at extreme hole doping a state with only  $\Delta_{e2}$  nonzero is realized, corresponding to the weak asymmetry seen in the  $T_{SDW}$  vs  $n_{el}$  curve in Fig. 3(b).

## V. ORTHORHOMBIC DISTORTION

In all known FeAs parent compounds, the SDW phase occurs only in the presence of an orthorhombic distortion of the crystal. It is found that the stripe-like SDW has its nesting vector  $\mathbf{Q}$  oriented along the longer crystal axis.<sup>3,4</sup> Here we see how this can be understood within our model on the basis of the effect of the orthorhombic distortion on the Fermi surfaces.

Under an orthorhombic distortion, the energy shift of a state with wave vector  $\mathbf{K}$  in the unfolded Brillouin zone is  $\delta\epsilon_{\mathbf{K}} \sim \sum_{\alpha,\beta} K_{\alpha} Y_{\alpha,\beta} K_{\beta}$  where  $Y_{\alpha,\beta}$  is the strain tensor and we have  $Y_{xx} = -Y_{yy}$  and  $Y_{xy} = 0$ .<sup>26</sup> Note that the wave vectors  $\mathbf{K}$  in the unfolded Brillouin zone are rotated by  $45^\circ$  with respect to the wave vectors in the crystallographic Brillouin zone. We approximate the energy shifts  $\delta\epsilon_{\mathbf{K}}$  by their value near the chemical potential as the Fermi surface shape dominates the physics of our model. The energy shifts of the hole states near the zone center are therefore neglected as they will be much smaller than those experienced by the electron pockets. Since the electron pockets are small, we assume that their energy shifts are isotropic. Furthermore, the sign of the energy shift will be opposite for the electron pockets at the  $X$  points along the axes of compression (negative energy shift) and dilation (positive energy shift).<sup>26</sup> We hence model the effect of the orthorhombic distortion by  $\epsilon_{n\mathbf{k}}^e \rightarrow \epsilon_{n\mathbf{k}}^e + (-1)^n \delta\epsilon$ . We compare the electron pockets at  $\delta\epsilon = 0.04$  eV and  $\delta\epsilon = 0$  in Fig. 4(a).

The dependence of the  $\Delta_{eh}$  on  $\delta\epsilon$  at  $T = 1$  K and  $T = 40$  K is plotted in Figs. 4(b) and 4(c), respectively. The

effect of  $\delta\epsilon \neq 0$  is to enhance the pairing between the larger electron and hole pockets ( $\Delta_{11}$ ) and also the smaller electron and hole pockets ( $\Delta_{22}$ ) while suppressing the pairing between the smaller electron (hole) and larger hole (electron) pockets. In analogy to the effect of doping, this can be readily understood as due to the changes in the area enclosed by each electron Fermi surface. Due to the enhanced excitonic pairing, the free energy  $F$  shows monotonic decrease with increasing  $\delta\epsilon$  [see Fig. 4(d)]. As the orthorhombic distortion should increase the elastic energy of the lattice, it is therefore possible that the total free energy of the crystal will show a minimum at a nonzero value of the distortion. Deeper investigation of this scenario is left for future work.

The  $T=40$  K case shows a large range of  $\delta\epsilon$  where  $\Delta_{11}$  is the only nonzero excitonic average; i.e., the distortion stabilizes a single- $\mathbf{Q}$  SDW state due to the enhanced nesting between the larger electron and hole pockets. In contradiction to experiment, however, the  $\mathbf{Q}$  vector is oriented along the shorter crystal axis. This does not necessarily invalidate the excitonic scenario: our model [Eq. (1)] has equal coupling constants between the different bands. If hole band 2 was to interact more strongly with the electron bands than hole band 1, so that  $|\Delta_{e2}| \gg |\Delta_{e1}|$  in the undistorted system, the enhancement (suppression) of  $\Delta_{22}$  ( $\Delta_{12}$ ) by the orthorhombic distortion would likely stabilize a SDW state with the observed  $\mathbf{Q}$  vector. For this, the required effective SDW coupling between the electron pockets and hole band 2 is  $\geq 1.1g_s$ , while the interaction with hole band 1 must be at most  $0.9g_s$ .

## VI. CONCLUSIONS

We have presented a mean-field study of the excitonic SDW state for a realistic four-band model of the FeAs parent compounds. We find that the SDW state is sensitively dependent on the band structure. For a tetragonal unit cell, a two- $\mathbf{Q}$  SDW is realized at  $n_{el}=4$ ; small changes in the electron pocket ellipticity or the doping, however, stabilize the observed single- $\mathbf{Q}$  state. Varying the relative size of the hole pockets qualitatively changes the  $T_{SDW}$  vs  $n_{el}$  curve, agreeing best with experiment when the hole pockets are almost coincident.<sup>1,3</sup> The dominant effect of an orthorhombic distortion of the crystal on the band structure was identified as altering the size of the electron pockets. This changes the nesting condition between the Fermi surfaces and can realize a single- $\mathbf{Q}$  SDW. Our analysis suggests that the electron pockets interact more strongly with the smaller hole Fermi surface than with the larger. We conclude that the excitonic SDW model is capable of qualitatively describing the AF phase of the FeAs parent compounds. The strong sensitivity of the SDW state on the band structure, however, shows that a quantitative description requires a more detailed understanding of the electronic structure than is currently available.

The authors thank I. Eremin and D. V. Efremov for useful discussions.

\*brydon@theory.phy.tu-dresden.de

†carsten.timm@tu-dresden.de

<sup>1</sup>Y. Kamihara *et al.*, *J. Am. Chem. Soc.* **130**, 3296 (2008).

<sup>2</sup>M. Rotter, M. Tegel, and D. Johrendt, *Phys. Rev. Lett.* **101**, 107006 (2008).

<sup>3</sup>J. Zhao *et al.*, *Nature Mater.* **7**, 953 (2008); J. Zhao *et al.*, *Phys. Rev. B* **78**, 132504 (2008).

<sup>4</sup>Q. Huang, Y. Qiu, W. Bao, M. A. Green, J. W. Lynn, Y. C. Gasparovic, T. Wu, G. Wu, and X. H. Chen, *Phys. Rev. Lett.* **101**, 257003 (2008); A. Jesche *et al.*, *Phys. Rev. B* **78**, 180504(R) (2008).

<sup>5</sup>M. A. McGuire *et al.*, *Phys. Rev. B* **78**, 094517 (2008); M. A. McGuire *et al.*, *New J. Phys.* **11**, 025011 (2009).

<sup>6</sup>W. Z. Hu, J. Dong, G. Li, Z. Li, P. Zheng, G. F. Chen, J. L. Luo, and N. L. Wang, *Phys. Rev. Lett.* **101**, 257005 (2008).

<sup>7</sup>S. E. Sebastian *et al.*, *J. Phys.: Condens. Matter* **20**, 422203 (2008).

<sup>8</sup>D. Hsieh *et al.*, arXiv:0812.2289 (unpublished).

<sup>9</sup>I. I. Mazin, D. J. Singh, M. D. Johannes, and M. H. Du, *Phys. Rev. Lett.* **101**, 057003 (2008).

<sup>10</sup>D. J. Singh and M.-H. Du, *Phys. Rev. Lett.* **100**, 237003 (2008).

<sup>11</sup>M. M. Korshunov and I. Eremin, *Europhys. Lett.* **83**, 67003 (2008); *Phys. Rev. B* **78**, 140509(R) (2008).

<sup>12</sup>T. M. Rice, *Phys. Rev. B* **2**, 3619 (1970).

<sup>13</sup>K. Kuroki, S. Onari, R. Arita, H. Usui, Y. Tanaka, H. Kontani, and H. Aoki, *Phys. Rev. Lett.* **101**, 087004 (2008).

<sup>14</sup>J. Lorenzana, G. Seibold, C. Ortix, and M. Grilli, *Phys. Rev.*

*Lett.* **101**, 186402 (2008).

<sup>15</sup>Y. Ran, F. Wang, H. Zhai, A. Vishwanath, and D. H. Lee, *Phys. Rev. B* **79**, 014505 (2009).

<sup>16</sup>R. Yu, K. T. Trinh, A. Moreo, M. Daghofer, J. A. Riera, S. Haas, and E. Dagotto, *Phys. Rev. B* **79**, 104510 (2009).

<sup>17</sup>Q. Han, Y. Chen, and Z. D. Wang, *Europhys. Lett.* **82**, 37007 (2008).

<sup>18</sup>A. V. Chubukov, D. V. Efremov, and I. Eremin, *Phys. Rev. B* **78**, 134512 (2008).

<sup>19</sup>A. B. Vorontsov, M. G. Vavilov, and A. V. Chubukov, *Phys. Rev. B* **79**, 060508(R) (2009).

<sup>20</sup>L. V. Keldysh and Y. V. Kopaev, *Sov. Phys. Solid State* **6**, 2219 (1965); *J. des Cloiseaux, J. Phys. Chem. Solids* **26**, 259 (1965).

<sup>21</sup>Y. V. Kopaev, *Sov. Phys. Solid State* **12**, 1 (1970).

<sup>22</sup>D. W. Buker, *Phys. Rev. B* **24**, 5713 (1981).

<sup>23</sup>The correlated transition term may also play a role in the superconductivity of the FeAs compounds (see Ref. 18); V. Barzykin and L. P. Gor'kov, *JETP Lett.* **88**, 131 (2008); L. Benfatto, M. Capone, S. Caprara, C. Castellani, and C. Di Castro, *Phys. Rev. B* **78**, 140502(R) (2008).

<sup>24</sup>I. I. Mazin and M. D. Johannes, *Nat. Phys.* **5**, 141 (2009).

<sup>25</sup>L. Ortenzi *et al.*, arXiv:0903.0315 (unpublished) have shown that strong interband coupling can cause such a shift due to correlation effects beyond the mean-field approximation.

<sup>26</sup>S. C. Hunter and F. R. N. Nabarro, *Proc. R. Soc. London, Ser. A* **220**, 542 (1953); J. M. Ziman, *Electrons and Phonons* (Oxford University Press, Oxford, 1960).